Journal of Photochemistry and Photobiology A: Chemistry 348 (2017) 295–304

Contents lists available at ScienceDirect

Journal of Photochemistry and Photobiology A: Chemistry

journal homepage: www.elsevier.com/locate/jphotochem

Invited feature article

Cyclodextrine-nanoencapsulation of niclosamide: Water solubility and meaningful enhancement of visible-light—Mediated sensitized photodegradation of the drug

Eduardo Gatica[a], José Natera[a,*], Adriana Pajares[b,c], Carolina Gambetta[a], Matías I. Sancho[d], Walter A. Massad[a], Norman A. García[a,*]

[a] Departamento de Química, Universidad Nacional de Río Cuarto, 5800 Río Cuarto, Argentina
[b] Facultad de Ingeniería Universidad Nacional de la Patagonia SJB, 9000 Comodoro Rivadavia, Argentina
[c] Unidad Académica Río Gallegos, Universidad Nacional de la Patagonia Austral, 9400 Río Gallegos, Argentina
[d] IMIBIO – CONICET – Fac.de Química, Bioquímica y Farmacia, Área de Química Física, UNSL, 5700 San Luis, Argentina

ARTICLE INFO

Article history:
Received 11 May 2017
Received in revised form 13 July 2017
Accepted 8 August 2017
Available online 24 August 2017

Keywords:
Cyclodextrin encapsulation
Niclosamide
Photooxidation
Photosensitization
Reactive oxygen species
Riboflavin

ABSTRACT

A kinetic and mechanistic study of the daylight-mediated photooxidation of the multifunctional drug Niclosamide (NSD) was carried out in aqueous solutions. NSD is a frequent contaminant suspended in natural waters. The aqueous dissolution of the practically insoluble NSD was driven by the presence of 2-hydrxypropyl-β-cyclodextrin (HPβCD). The already proposed formation of an inclusion complex between NSD-HPβCD was confirmed through theoretical studies. NSD-nanoencapsulation within the oligosaccharide occurs with a 1:2 stoichiometry, being the drug embedded into a cavity of two HPβCD molecules, in a so called head-to-head orientation.

The Reactive Oxygen Species singlet molecular oxygen, superoxide radical anion and hydrogen peroxide, generated through the visible-light absorber sensitizers Riboflavin and Rose Bengal, are effectively intercepted by the encapsulated biocide and contribute to its photodegradation. The overall NSD photooxidation rate, determined through oxygen consumption indicates that the process is relatively highly efficient in the microheterogeneous aqueous media as compared to NSD in MeOH solution, and to phenol (PHE) in pure water. The paradigmatic water-contaminant PHE was taken a as reference in order to evaluate the persistence of the NSD under photosensitized irradiation in aqueous medium. The photooxidation mechanism of NSD is affected by cyclodextrin complexation, due to dynamic limitations, electrostatic interactions and pH changes upon NSD dissolution in aqueous HPβCD. In this sense, the NSD-HPβCD complex can be seen as a sort of nanoreactor that enables the photodegradation of the biocide in water, under daylight conditions.

1. Introduction

Niclosamide (5-Chloro-N-(2-Chloro-nitrophenyl)-2-hydroxy-benzamide, NSD), a water-insoluble multifunctional drug, widespread employed as a biocide is frequently found as a contaminant, suspended in surface waters [1].

Considering the environmental relevance of light-induced degradative processes, a kinetic and mechanistic study of the daylight-mediated photooxidation of NSD, in methanolic solution, has been recently undertaken by ourselves [2]. The mentioned research work was important as an initial approximation towards the possible natural fate of the contaminant in solution, under daylight photoirradiation. Riboflavin (Rf, vitamin B2) was employed as photosensitizer. The vitamin constitutes an archetypal natural photosensitizer, profusely employed to model the oxidative photodegradation of numerous water contaminants [3–5]. The reactive oxygen species (ROS) singlet molecular oxygen ($O_2(^1\Delta_g)$) and superoxide radical anion ($O_2^{\bullet}-$) were responsible for the NSD photodegradation. Nevertheless, the use of a non-natural solvent, such as MeOH, in a study on contaminated waters, constitutes an approach that, from the environmental point of view, deserves to be improved.

In the present work we attempt to overcome the limited NSD water-solubility by means of the employment of cyclodextrins (CD). It is known that these oligosaccharides form macrocycles

* Corresponding authors.
E-mail addresses: jnatera@exa.unrc.edu.ar (J. Natera), ngarcia@exa.unrc.edu.ar (N.A. García).

http://dx.doi.org/10.1016/j.jphotochem.2017.08.015
1010-6030/

joined by glycosidic linkages whose hydrophobic inner space and hydrophilic external surface offers the possibility to form inclusion complexes with different liposoluble substrates, in a kind of "host-guest" association [6].

It is also well known that the inclusion of a given hydrophobic substrate into a cyclodextrin cavity frequently leads to physicochemical changes on the guest substrate. These changes are not only limited to effects on water solubility. They can also affect the chemical behavior of the encapsulated molecule towards different physicochemical stimulations, including photoinduced reactivity [6–9].

All these considerations sparked our interest in the re-evaluation of the Rf-photosensitized degradation of NSD, performed in the presence of aqueous 2-hydrxypropyl-β-cyclodextrin (HPβCD). This oligosaccharide was chosen because it has been reported that, although the vitamin and HPβCD forms a hydrogen-bonded noninclusion complex, with a stability constant of 5.75 M^{-1}, the association does not produce noticeable modifications in the physicochemical properties of Rf. [10].

In the present study, the formation of inclusion complexes between NSD and HPβCD, already experimentally examined by Devarakonda et al. [11], was systematically characterized through theoretical studies. Following, the effect of such an association on the kinetic and mechanistic aspects of Rf-sensitized NSD photodegradation was evaluated, under visible light irradiation. Results clearly show significant changes in the photodegradation rate of the contaminant as compared to what we found in methanolic homogeneous medium [2].

Summarizing, the present work addresses two important topics: (a) The physicochemical understanding of CD-inclusion complexes with environmentally relevant molecules and (b) The influence on water-solubility on the efficiency of NSD daylight-mediated photodegradation.

In addition to the environmental importance of the research work, the combined results also lead to the possibility of optimizing the efficiency of low-energy demanding reactors for remediation of stored residual waters containing water-insoluble suspended contaminants.

2. Experimental

2.1. Materials

Riboflavin, the proteins catalase (CAT, from bovine liver) and superoxide dismutase (SOD; from bovine erythrocytes) were purchased from Sigma Chem. Co. Furfuryl acetate (FFAc) and phenol were purchased from Sigma Chem. Co., Rose Bengal (RB), deuterium oxide (D_2O; 99.9 atom% D) were from Aldrich. (2-Hydroxypropyl)-β-cyclodextrin, average M_w ~1541.56 was from Sigma-Aldrich.

2.2. Apparatus and methods

In all the cases, pHs/pDs were controlled with a MP220 Mettler-Toledo pH-meter.

Ground state absorption spectra were registered in a Hewlett Packard 8453 diode array spectrophotometer.

2.2.1. Continuous photolysis

Continuous aerobic photolysis of aqueous solutions containing the substrates plus sensitizers were carried by means of blue leds (for Rf-sensitization) and green leds (for RB-sensitization) with irradiation wavelengths of 465 ± 25 nm and 510 ± 40 nm respectively. Oxygen uptake experiments were performed employing a home-made photolyser provided with a quartz-halogen lamp (150-W) and a cut-off filter at 450 nm.

The reactive rate constant, k_r, for the chemical reaction of $O_2(^1\Delta_g)$ (see further process ((13) in Scheme 2) was evaluated as described by Scully and Hoigné [12], using the expression slope/$slope_R = k_r$ [NSD-HPβCD]/k_{rR} [R]. In this case the knowledge of the rate constant value (k_{rR}) for the photooxidation of a reference compound R, is required. Slope and $slope_R$ represent the slopes of

$$\text{Rf- HP}\beta\text{CD} + h\nu \rightarrow {}^1\text{Rf- HP}\beta\text{CD}^* \rightarrow {}^3\text{Rf- HP}\beta\text{CD}^* \quad (5)$$

$${}^3\text{Rf- HP}\beta\text{CD}^* + \text{NSD-(HP}\beta\text{CD)}_2 \rightarrow \text{Rf- HP}\beta\text{CD}^{\bullet-} + \text{NSD-(H}\beta\text{PCD)}_2^{\bullet+} \quad (6)$$

rate constant k_{q3}

$$\text{Rf- HP}\beta\text{CD}^{\bullet-} + \text{H}^+ \rightarrow \text{RfH- HP}\beta\text{CD}^{\bullet} \quad (7)$$

$$2\ \text{RfH-HP}\beta\text{CD}^{\bullet} \rightarrow \text{Rf} + \text{RfH}_2\text{- HP}\beta\text{CD}_2 \quad (8)$$

$$\text{RfH}_2\text{- HP}\beta\text{CD} + O_2({}^3\Sigma_g^-) \rightarrow \text{RfH}_2\text{- HP}\beta\text{CD}^{\bullet+} + O_2^{\bullet-} \quad (9)$$

$$O_2^{\bullet-} + \text{NSD-(HP}\beta\text{CD)}_2 \rightarrow \text{P10} \quad (10)$$

$$\text{RfH}_2\text{-HP}\beta\text{CD}^{\bullet+} + O_2^{\bullet-} \rightarrow \text{Rf} + H_2O_2 \quad (11)$$

$$H_2O_2 + \text{NSD-(HP}\beta\text{CD)}_2 \rightarrow \text{P(12)} \quad (12)$$

$${}^3\text{Rf- HP}\beta\text{CD}^* + O_2({}^3\Sigma_g^-) \rightarrow \text{Rf-HP}\beta\text{CD} + O_2({}^1\Delta_g) \quad (13)$$

rate constant k_{ET}

$$O_2({}^1\Delta_g) \rightarrow O_2({}^3\Sigma_g^-) \quad (14)$$

rate constant k_d

$$O_2({}^1\Delta_g) + \text{NSD-(HP}\beta\text{CD)}_2 \rightarrow O_2({}^3\Sigma_g^-) + \text{NSD-(HP}\beta\text{CD)}_2 \quad (15)$$

rate constant k_q

$$O_2({}^1\Delta_g) + \text{NSD-(HP}\beta\text{CD)}_2 \rightarrow \text{P16} \quad (16)$$

rate constant k_r

Being $k_r + k_q = k_t$

Scheme 1. Possible pathways for a Rf- HPβCD – sensitized process in the presence of a hypothetical electron donor (NSD), transparent to the photoirradiation wavelength. For simplicity, natural decay processes from the species ^{1}Rf- HPβCD* and ^{3}Rf- HPβCD* have been ignored.

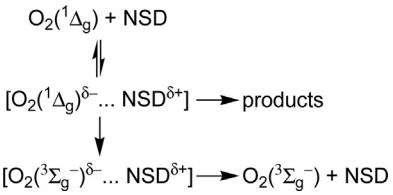

Scheme 2. Generation and evolution of the encounter excited complex between $O_2(^1{}_g)$ and a NSD. For simplicity NSD represents NSD-$(HP\beta CD)_2$.

the first-order plots of substrate and the reference compound respectively, under photosensitization, being [NSD-HPβCD] = [R]. The reference R was FFAc, with a k_{rR} value in water of $8.6 \times 10^7\ M^{-1}\ s^{-1}$.

Oxygen uptake in water was monitored employing a 97-08 Orion electrode.

2.2.2. Laser flash photolysis experiments

N_2-saturated aqueous solutions of 0.03 mM Rf plus 37 mM HPβCD were irradiated with a flash photolysis apparatus. A ns Nd:YAG laser system (Spectron) at 355 nm was used as an excitation source. The analyzing light was a 150-W Xenon lamp. A PTI (Photon Technology International) device was employed for the detection system, constituted by a monochromator and a red-extended photomultiplier (Hamamatsu R666). The signal was acquired and averaged by a digital oscilloscope (Hewlett-Packard 54504A). It was transferred, by means of a HPIB parallel interface, to a personal computer where the signal was analyzed and stored. The disappearance of the species generated by the 355 nm pulse (^{3}Rf*) was monitored through the absorbance first-order decay at 670 nm. In this wavelength zone the interference from other possible species is negligible. The decay was measured at low enough laser energy and Rf concentration as low as possible, in order to avoid hindering process as self-quenching or triplet–triplet annihilation.

NSD presents a relatively strong absorption at 355 nm, which is the excitation wavelength employed to generate triplet excited Rf (^{3}Rf*) in our LFP apparatus. Hence, the relatively high NSD concentration necessary to quench almost completely ^{3}Rf*, in order to obtain the spectrum of the transient species derived from Rf in such a condition, precludes the observation of any transient spectrum. Even so, it was possible in this case the evaluation of the k_{q3} value (process (6), see further Scheme 1) through a Stern-Volmer treatment. In this case a relatively low NSD concentration is required to reach a sufficiently measurable quenching of ^{3}Rf*.

2.2.3. Time resolved phosphorescence detection (TRPD) of $O_2(^1\Delta_g)$

The overall quenching rate constant for the deactivation of $O_2(^1\Delta_g)$ by NSD-HPβCD (k_t, the sum of k_q plus k_r, processes (15) and (16), respectively, see latter Scheme 2) was determined using a previously reported system [13]. Briefly, a Nd:YAG laser (Spectron) was employed for the excitation (532 nm) of the sensitizer RB ($Abs_{532} = 0.4$), and the emitted radiation ($O_2(^1\Delta_g)$ phosphorescence at 1270 nm) was detected at right angles using an amplified Judson J16/8Sp germanium detector, after passing through two Wratten filters. The output of the detector was coupled to a digital oscilloscope and to a personal computer for the signal processing. Usually, 16 shots were needed for averaging, so as to achieve a good signal to noise ratio, from which the decay curve was obtained. Air-saturated solutions were employed in all the cases. In the dynamic determinations, D_2O, instead of H_2O, was used as a solvent in order to enlarge the lifetime of $O_2(^1\Delta_g)$ [14].

2.3. Molecular modeling

A relaxed potential energy surface was calculated at PM6 (Parametric Model 6) level of theory on the molecular geometry of NSD [15]. The scanned parameter was the dihedral angle ω in a 0°–360° range, with a step size of 10° (Fig. 1).

The most stable conformer was further optimized at the B3LYP/6-31 + G(d,p) level of theory. The βCD geometry was constructed using crystallographic data and then, taking into account the degree of substitution of the HPβCD used in the experimental work, the hydroxypropyl (HP) groups were added on βCD [16]. According to experimental data two possible stoichiometries were

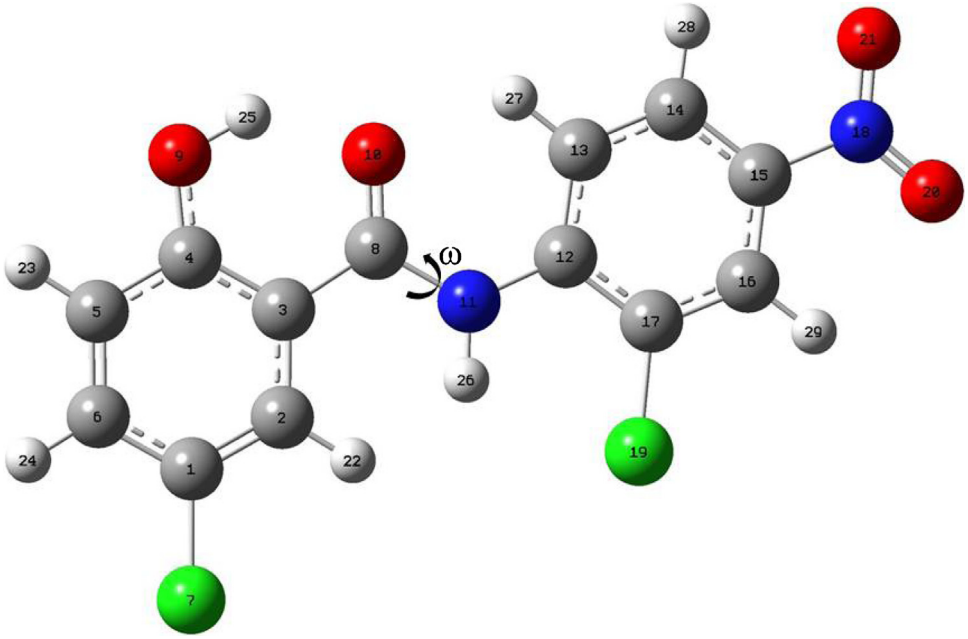

Fig. 1. Molecular structure, torsional angle (ω) and practical numbering system of niclosamide adopted for the calculations. Color references: gray = carbon, red = oxygen, blue = nitrogen, green = chlorine and white = hydrogen. (For interpretation of the references to color in this figure legend, the reader is referred to the web version of this article.)

considered to simulate the inclusion process, a 1:1 and a 1:2 NSD-HPβCD complex. For the 1:1 complex, a known procedure was followed to simulate the inclusion process [17], and two possible orientations were considered: the "Head Down" and "Head Up" orientations, in which NSD initially points toward the HP groups and the hydroxyls of βCD, respectively. A total of 17 possible structures were used as starting points for each orientation. For the 1:2 complexes, the same procedure was followed using four different orientations as starting points for the simulations (Fig. 2).

All the inclusion complexes structures generated with this scheme were fully optimized using the PM6 method. Then, the most stable geometry of each orientation (for both stoichiometries) was further optimized with the hybrid two-layer ONIOM methodology. [18] The PM6 method was employed to model the HPβCD and the DFT B3LYP/6-31 + G(d,p) level of theory was used for the NSD molecule. A Natural Bond Orbital (NBO) analysis was performed on these structures at the B3LYP 6-31 + G(d,p) level of theory, in order to quantify relevant interactions in the inclusion complexes. All the calculations were performed with GAUSSIAN 09 software packages [19].

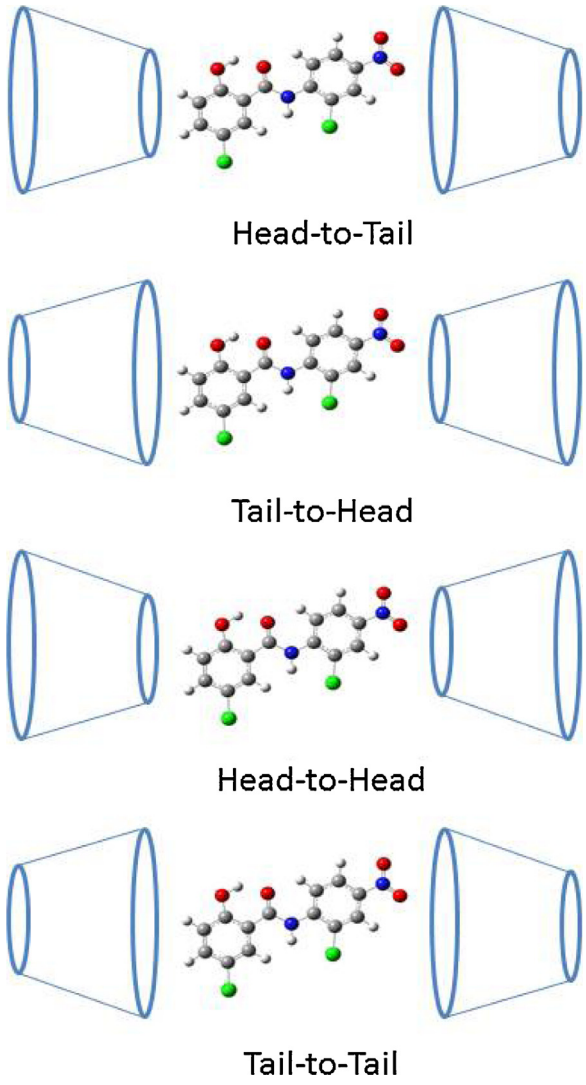

Fig. 2. Orientations of NSD and HPβCD in the 1:2 complexes adopted for the quantum chemical calculations.

3. Results

3.1. The formation of HPβCD-NSD inclusion complex. Comparison of experimental results and theoretical calculations

The solubilization of NSD by HPβCD has been studied by Devarakonda et al. [11] The authors were interested in problems associated with the successful preparation of pharmacological products in aqueous solution, able to include the practically insoluble NSD. They reported a significant increase of NSD solubility in the presence of HPβCD, attributed to physical changes in the drug upon HPβCD-complexation, with 1:1 and 1:2 NSD-HPβCD complex-stoichiometry. The experimentally determined equilibrium stability constants, for the processes represented in Eqs. (1) and (2) were $Ka_{1:1} = 20.16\,M^{-1}$ and $Ka_{1:2} = 342.06\,M^{-1}$ respectively

$$NSD + HP\beta CD \leftrightarrows NSD\text{-}HP\beta CD \quad (1)$$

$$NSD\text{-}HP\beta CD + HP\beta CD \leftrightarrows NSD\text{-}(HP\beta CD)_2 \quad (2)$$

In order to go deeper in the understanding of the complexation of the system NSD + HPβCD, the molecular structure of the inclusion complexes was investigated using computational chemistry methods.

The stabilization energy of the inclusion process (ΔE) was calculated with the PM6 method as follows:

$$\Delta E = E_{complex} - (E_{NSD} + n\ E_{\ HP\beta CD}) \quad (3)$$

In the case of the 1:1 stoichiometry ($n = 1$ in Eq. (3)) two possible orientations were considered for the inclusion complex, the head up and head down. The results of the calculations are reported in Table 1.

It can be observed that the head up orientation is energetically favorable by 4 kJ/mol approximately. This energy difference is increased at 22 kJ/mol when is calculated with the ONIOM(B3LYP/6-31G(d,p):PM6) level of theory. The molecular structure of minimum energy obtained with the ONIOM methodology is illustrated in Fig. 3.

It can be observed that the NSD molecule is not completely embedded into HPβCD, and the salicylamide moiety remains outside the cavity. For the 1:2 stoichiometry, four possible orientations were considered for the inclusion complex (Fig. 2). The PM6 results ($n = 2$ in Eq. (3)) indicated that the lowest energy complex is obtained with the orientation called "head-to-head". In this configuration, the HPβCD rims with OH groups are pointing toward the NSD molecule while the rims with the HP groups are pointing to the outside of the complex. This orientation is also the most stable conformation according to the ONIOM calculations (see Table 1). The ΔE(ONIOM) reported in this table is calculated

Table 1
Energy differences of the NSD inclusion complexes with 2HPβCD in kJ/mol. ΔE (PM6) is the stabilization energy calculated according to Eq. (3) while ΔE (ONIOM) is the energy difference between the most stable orientation of each complex and the rest the orientations considered in the ONIOM(B3LYP/-31 + G(d,p):PM6) calculations.

Complex	ΔE (PM6)	ΔE (ONIOM)
NSD:HPβCD		
Head Up	−82.29	0
Head Down	−78.41	22.03
NSD:$(HP\beta CD)_2$		
Head-to-Tail	−183.29	20.22
Tail-to-Head	−183.91	31.48
Head-to-Head	−213.06	0
Tail-to-Tail	−173.52	38.31

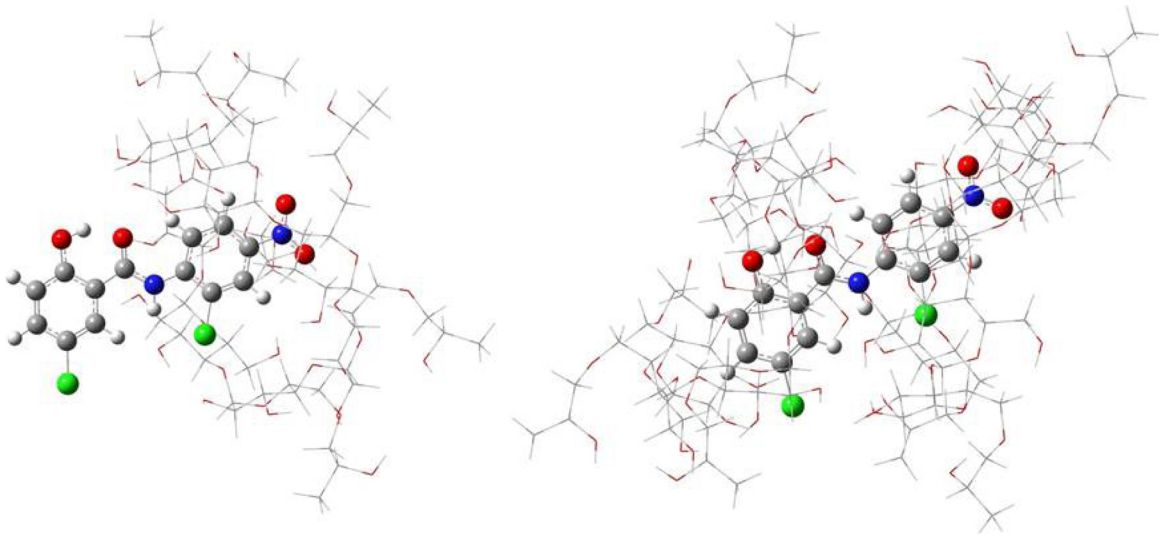

Fig. 3. Molecular structures of the 1:1 (left) and 1:2 (right) NSD:HPβCD inclusion complexes calculated with the ONIOM(B3LYP/6-31 + G(d,p):PM6) methodology.

for a given orientation as the energy difference between the given complex and the energy of the most stable complex. The tail-to-tail orientation (the HP of both CDs are oriented towards the NSD molecule) presents the least stable structure of the four orientations proposed, and the other two orientations exhibit intermediate energies. These results suggest that the complexation of NSD with HPβCD is favored when the drug interacts with the OH groups of CD and the HP groups are facing outside the complex.

In order to quantify the strength of relevant intermolecular interactions between NSD and HPβCD a NBO analysis was performed on the most stable structures of 1:1 and 1:2 complexes. The stabilization energy (ΔE_{ij}) was calculated using the following equation:

$$\Delta E_{ij} = \frac{q_i F_{ij}}{(\varepsilon_j - \varepsilon_i)} \quad (4)$$

Where q_i is the donor orbital occupancy, ε_i and ε_j are the energies of the interacting orbitals, and F_{ij} is the off-diagonal NBO Fock matrix element [20]. The calculated ΔE_{ij} values are useful to estimate the energy of a donor-acceptor interaction, and for an H-bond, the donor is a lone pair (LP) of one electronegative atom (O or N) and the acceptor is the antibonding (σ*) orbital of OH or NH groups. Table 2 shows the calculated values of ΔE_{ij}, $(\Phi_j - \Phi_i)$ and F_{ji} for the 1:1 and 1:2 inclusion complexes of NSD with HPβCD. Φ

Only one intermolecular H-bond is observed in the 1:1 complex between the amidic N-H of NSD and a glycosidic oxygen of HPβCD. The bond length and bond angle of this interaction is 2.15 Å and 146°, respectively. On the other hand, four intermolecular H-bonds were detected for the 1:2 complex, where the interaction between the amidic N-H and the glycosidic oxygen is also the most stable one. In this case, the bond length and bond angle of this interaction is 2.18 Å and 136°, respectively. In addition to the H-bonds, a weak non-covalent interaction between a chlorine atom and one H of the CD was also observed.

This kind of interaction has been previously reported for other CD inclusion complexes [21,22].

Table 2
Results of the NBO analysis for the 1:1 and 1:2 NSD:HPβCD inclusion complexes at B3LYP 6-31 + G(d,p) level of theory.

NSD:HPbCD	Φi	Φj	ΔE_{ij}/kJ · mol^{-1}	εj-εi/a.u	F_{ij}/a.u
01:01	$LP_2\ (O_{49})_{CD}$	$\sigma^*\ (N_{11}H)_{NSD}$	37.26	0.77	0.069
	$LP_1(O_{21})_{NSD}$	$\sigma^*\ (OH)_{CD}$	12.18	1.21	0.049
	$LP_2(O_{21})_{NSD}$	$\sigma^*\ (OH)_{CD}$	12.85	0.72	0.04
01:02	$LP_2\ (O_{27})_{CD}$	$\sigma^*\ (N_{11}H)_{NSD}$	22.1	0.74	0.052
	$LP_1(O_{10})_{NSD}$	$\sigma^*\ (OH)_{CD}$	13.48	0.72	0.04
	$LP_2(Cl_7)_{NSD}$	$\sigma^*\ (OH)_{CD}$	18.53	0.7	0.046

Note: Φ*i* and Φ*j*: donor and acceptor orbitals, respectively, LP: lone pair orbitals, σ*: antibonding orbitals, ΔE_{ij}: second order stabilization energy, $\varepsilon_j - \varepsilon_i$: energy difference of the interacting orbitals, F_{ij}: off-diagonal NBO Fock matrix element.

3.2. Experimental conditions of NSD solubilization in HPβCD solution

A concentration of 37 mM was the lowest HPβCD concentration able to dissolve *ca.* 0.07 mM NSD in aqueous solution. In the following we will refer to this mixture as NSD-$(HP\beta CD)_2$ or NSD-HPβC complex. The pH of the water employed was 6.1 whereas in the presence of HPβCD (*ca.* 5% w/w) the pH was 7.1. This effect of increasing pH of water in the presence of hydroxypropyl cyclodextrins has been already observed for 2-hydrxypropyl-γ-cyclodextrin. Values between 7 and 9 have been found for a 2% w/w aqueous solution of this compound [23].

The absorption spectrum of NSD in the UVA region presents two bands in MeOH, centered approximately at 325 (band I) and 385 nm (band II) (Fig. 4). They correspond to the unionized and ionized phenolic forms of NSD respectively ($pK_a = 7.3$) [10]. In pure

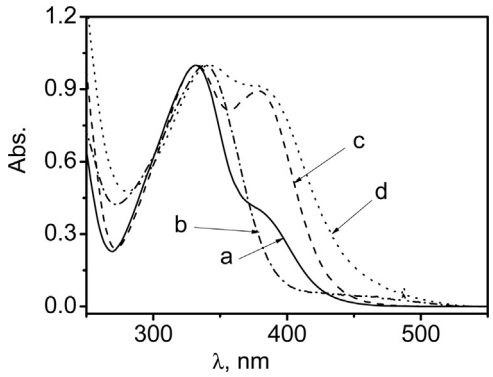

Fig. 4. UV–vis absorption spectra of NSD in different media. (a) NSD in MeOH; (b) NSD in MeOH/0.05 mM HCl; (c) NSD in MeOH/0.05 mM NaOH; (d) NSD-$(HP\beta CD)_2$ in aqueous solution with 0.07 mM NSD and 37 mM HPβCD. All spectra were taken *vs.* the respective solvent. In order to facilitate visual comparison, the respective maxima of the absorption band of spectra (a), (b) and (c) in the range 320–345 nm have been normalized to the absorbance of spectrum (d) at 345 nm.

MeOH the ratio band I/band II is approximately 2.2 whereas in the same solvent but in the presence of 50 mM NaOH, the ratio is practically 1. The latter value remains unchanged upon addition of higher concentrations of alkali. This means that the spectral shape corresponds to the totally ionized form of NSD in MeOH, in agreement with the normal behavior expected for a typical phenolic derivative: the decrease of band I and the increase of band II as the pH of the medium increases. The absorption spectrum for NSD-(HPβCD)$_2$ in water, is quite similar to that of NSD in alkaline MeOH. The absorption spectrum of NSD in pure MeOH, corresponding to the unionized form is only reached at very low pH values for the system HPβCD-NSD, as in the presence of HCl ca. 0.05 mM (Fig. 4).

The pH of the HPβCD aqueous solution was 7.1 and 7.05 in the absence and in the presence of 0.07 mM NSD respectively. Being the phenolic NSD pK = 7.3 [11], practically half of the NSD molecules are in the phenolate form under work conditions.

In Fig. 4 the spectral shapes for methanolic NSD and aqueous NSD-HPβCD solutions in the ne presence and in the absence of HCl and NaOH are shown. All absorption spectra were normalized at 330 nm.

3.3. Photodegradation kinetics

The Rf-sensitized photoirradiation of air-equilibrated aqueous solutions of HPβCD −Rf —NSD with blue leds produces changes in the spectral region of the NSD absorption and also in the absorption bands of the sensitizer. This is shown in Fig. 5, main. The most pronounced spectral changes in the NSD component are observed in a short range around 390 nm. Fig. 5, Inset A, shows the spectral changes for Rf in the absence of NSD. It can be observed that in this case, no changes at all can be detected at 390 nm. Hence, the spectral modifications in the main figure at this wavelength should be attributed to chemical changes in NSD. This is clearly reflected in inset B of Fig. 5, by comparing the absorbance time-evolution monitored at 390 nm for the system HPβCD-Rf in the presence and in the absence of NSD. In the second case the spectral changes are negligible, even when monitored at prolonged irradiation time.

No changes at all were observed in the absorption spectrum of aqueous NSD-(HPβCD)$_2$ solution with 0.07 mM NSD and 37 mM HPβCD when photolyzed with blue leds in the absence of Rf, even when photoirradiation times higher than 2000 s were employed.

Parallel runs upon photoirradiation of the mentioned solutions containing the mixture HPβCD-Rf-NSD gave rise to oxygen consumption (Fig. 6, trace (a). Traces (b) and (c) will be analyzed further here).

All this experimental evidence points in the same direction that our previous results in homogeneous methanolic medium [2] under selective photoirradiation of Rf, the overall interaction Rf-NSD could include the participation of electronically excited states of the vitamin and the possible participation of reactive oxygen species (ROS) formed in the medium. Hence, results will be presented and discussed using a reaction scheme similar to the already employed in a previous paper, on the assumption that the involved reactive species could be closely the same to those identified in homogeneous medium. The only difference in the present case are the presence of the HPβCD associated with Rf instead of the free vitamin as a photosensitizing agent and NSD included in a HPβCD-complex. Scheme 1 constitutes a self-defined series of reactions occurring upon Rf photoexcitation, being NSD an electron-releasing species. Eventual products for the respective reaction (n) are represented by P(n) and ground state molecular oxygen is symbolized as $O_2(^3\Sigma_g^-)$.

We have disregarded the participation of the species ^{1}Rf-HPβCD* due to its short lifetime, which was reported as 5 ns in water and 4.7 ns in aqueous β-cyclodextrin [3,24]. So, the only remaining possibilities are the reaction of NSD-(HPβCD)$_2$ with excited triplet Rf and/or with the eventual ROS photogenerated through steps (9), (11) and (13). These possibilities were systematically investigated, as follows:

3.4. LFP experiments and the interaction $^3Rf^*$-NSD

A spectrum similar to the expected one for ^{3}Rf* in pure water was observed after the laser pulse, in the presence of 37 mM. HβCD [25].

^{3}Rf* lifetime was neatly reduced by the presence of the mixture HPβCD-Rf-NSD in the mM concentration range, demonstrating the occurrence of an interaction between the encapsulated biocide and the triplet excited pigment. A value for the bimolecular rate constant $k_{q3} = 5.1 \times 10^7\ M^{-1}\ s^{-1}$ (process (6)) was graphically obtained as shown in Fig. 7, main. No significant changes in ^{3}Rf lifetime were observed in the presence of HPβCD in similar concentrations to those employed in the present work.

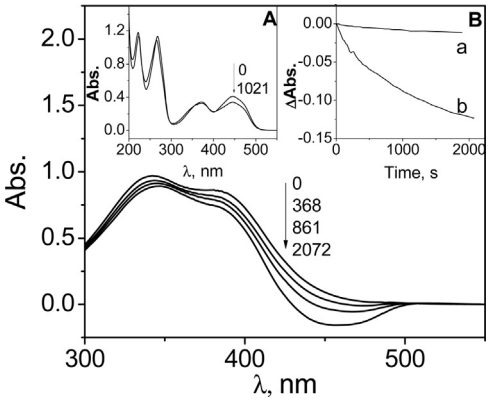

Fig. 5. changes in the UV–vis absorption spectra of an aqueous solution of NSD-(HPβCD)$_2$ containinig 0.07 mM NSD and 37 mM HPβCD plus Rf-HPβCD, containing 0.04 mM Rf and 37 mM HPβCD, *vs.* the described Rf-HPβCD (the whole mixture called solution I), upon photoirradiation. Inset A: changes in the UV–vis absorption spectra of an aqueous Rf-HPβCD containing 0.04 mM Rf and 37 mM HPβCD (solution II) *vs.* water, upon photoirradiation. Inset B: Temporal absorbance changes profiles monitored at 390 nm of solution II (a) and solution I upon photoirradiation. Actinic light: 465 ± 25 nm. Numbers on the spectra correspond to photoirradiation times (sec).

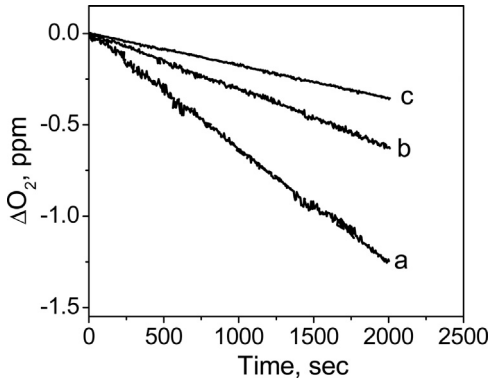

Fig. 6. Oxygen consumption as a function of photoirradiation time of the following aqueous solutions containing (a) NSD-(HPβCD)$_2$ containinig 0.07 mM NSD and 37 mM HPβCD plus Rf-HPβCD, containing 0.04 mM Rf and 37 mM HPβCD (the whole mixture called solution I). (b) Solution I plus 0.05 μM SOD. (c) Solution I plus 1 mg/100 ml CAT. Actinic light: 465 ± 5 nm.

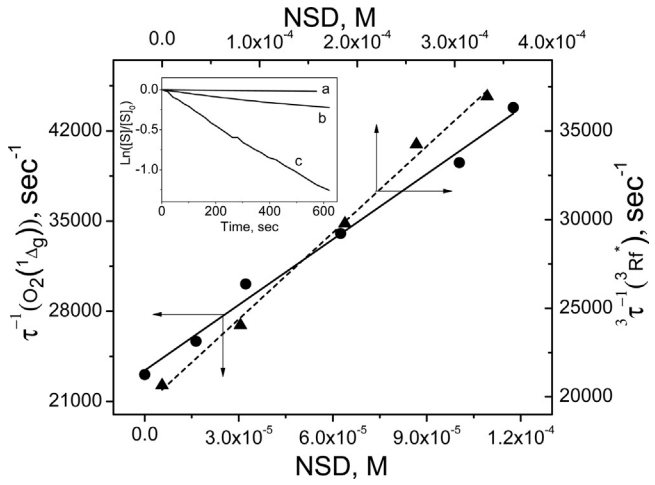

Fig. 7. (a) Stern-Volmer plot for the quenching of $O_2(^1\Delta_g)$ phosphorescence by NSD-$(HP\beta CD)_2$ in D_2O aerated solution plus 37 mM HPβCD. τ represents the $O_2(^1\Delta_g)$ phosphorescence lifetime. Photoexcitation at 532 nm. Sensitizer RB (A_{532} = 0.31). (b) Stern-Volmer plot for the evaluation of the rate constant for the quenching of $^3Rf^*$-HPβCD by NSD-$(HP\beta CD)_2$ in aqueous solution. Photoexcitation at 355 nm. Inset: First-order plots for substrate consumption upon the photoirradiation of the following aqueous solutions: (a) RB-HPβCD containing 0.009 mM RB plus 37 mM HPβCD (called solution I), monitored a 540 nm. (b) solution I plus NSD-$(HP\beta CD)_2$ containing 0.07 NSD and 37 mM HPβCD. (c) 0.07 mM FFAc pus 0.009 mM RB in water.

3.5. Possible involvement of ROS as oxidative agents

3.5.1. Quenching of $O_2(^1\Delta_g)$

All experiments involving possible $O_2(^1\Delta_g)$-mediated processes of the system NSD- HPβCD were performed in the presence of the exclusive $O_2(^1\Delta_g)$-generator dye RB. Rf was not employed in these experiments in order to prevent possible interferences by other potential ROS generated in the medium. RB is the sensitizer most frequently employed in $O_2(^1\Delta_g)$ reactions, with a reported quantum yield of 0.81 for $O_2(^1\Delta_g)$ production in water [26]. We compared the respective Φ_Δ values of RB in water and in water-HPβCD. Results, shown in Fig. 8, inset, indicate that the efficiency of $O_2(^1\Delta_g)$ generation in both media is closely the same. Photoirradiation with green leds of RB plus a NSD 0.07 mM in aqueous 37 mM HPβCD produces changes in the absorption spectrum of NSD, as shown in Fig. 8. The irradiation, even at light doses much higher than those employed in the experiment of Fig. 8, does not produce noticeable changes in the absorption spectrum of RB. According to Fini et al. the dye forms a 1:1 inclusion complex with HPβCD, for which an association constant of 140 M^{-1} has been reported [27].

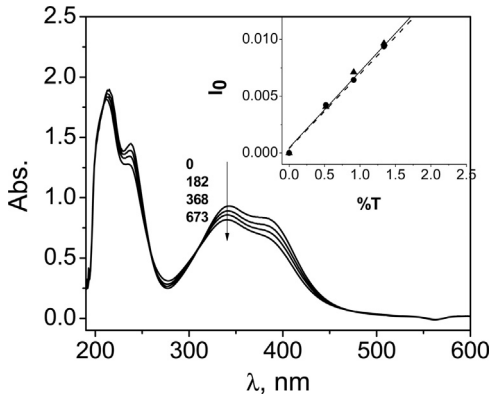

Fig. 8. changes in the UV–vis absorption spectra of an aqueous solution of NSD-$(HP\beta CD)_2$ containinig 0.07 mM NSD and 37 mM HPβCD plus RB-HPβCD containing 0.009 mM RB plus 37 mM HPβCD. Actinic light 510 ± 40 nm. Numbers on the spectra correspond to photoirradiation times (sec). Inset: Initial phosphorescence emission intensity of $O_2(^1\Delta_g)$ for the following aqueous solutions: (▲) 0.009 mM RB in water. (●) RB-HPβCD containing 0.009 mM RB and 37 mM HPβCD. Actinic light 532 nm.

The presence of NSD-$(HP\beta CD)_2$ in the sub-mM concentration range, produces the quenching of the IR phosphorescence emission of $O_2(^1\Delta_g)$ as detected by TRPD experiments. From the results shown in Fig. 7, (see above), arises a rate constant $k_t = 1.7 \times 10^8$ $M^{-1}s^{-1}$. This experiment constitutes an unambiguous evidence for the existence of an interaction $O_2(^1\Delta_g)$-NSD, which may be physical in nature (process (15)) and/or chemically reactive (process (16)). It is well known that the value *of* k_t, as determined by TRPD, does not rely on the type of sensitizer employed.

A rate constant value $k_r = 2.4 \times 10^7$ M^{-1} s^{-1}, was obtained by monitoring substrate consumption upon photoirradiation of the aqueous RB-HβCD-NSD mixtures, following the already described actinometric method [11]. Results are shown in Fig. 7, inset.

For comparative purposes, the respective rate constants for the $O_2(^1\Delta_g)$ quenching by the systems aqueous NSD-$(HP\beta CD)_2$, NSD in MeOH and NSD in alkalinized MeOH, the second and third values from our previous work [2], are shown in Table 1.

3.5.2. Participation of the ROS $O_2^{\bullet}-$ and H_2O_2

The individual presence of 0.05 μM SOD y 1×10^{-3} gr/100 ml CAT in an aqueous solution of Rf-NSD-HPβCD decreased the rate of oxygen photoconsumption as shown in Fig. 6. The enzymes have been currently employed to discard/confirm the participation of the species $O_2^{\bullet}-$ and H_2O_2 respectively in a given oxidative process. [28–30], SOD and CAT produce the dismutation of ROS as indicated by Reactions (17) and (18).

$$2\ O_2^{\bullet -} + 2H^+ + SOD \rightarrow O_2(^3\Sigma_g^-) + H_2O_2 \quad (17)$$

$$2\ H_2O_2 + CAT \rightarrow 2H_2O + O_2(^3\Sigma_g^-) \quad (18)$$

Results strongly suggest the participation of both ROS in the Rf-photosensitized photooxidation of HPβCD-included NSD.

3.6. The rates of oxygen photoconsumption by HPβCD-included NSD and aqueous PHE

Results shown up to this point are in agreement with the fact that Rf- and RB-sensitized photodegradation of HPβCD-encapsulated NSD occurs *via* ROS. Hence, in both cases the rates of oxygen uptake upon photosensitization (ROU) could be taken as an overall measure for photodegradation efficiency of the contaminant. On the basis that PHE is considered as an archetypal contaminant of surface waters, its ROU in aqueous solution was taken as a reference system. It is well known that PHE is also photooxidizable by ROS upon Rf and RB photosensitization [25]. In fact, literature reports on the Rf-sensitized photooxidation of PHE indicate that the main oxidative species is $O_2^{\bullet}-$, whereas $O_2(^1\Delta_g)$ is quenched in a dominant physical fashion [25].

Following, the ROU for aqueous Rf-HPβCD-NSD and RB-HPβCD-NSD were compared in individual relative terms to the respective ROU for aqueous Rf-PHE and aqueous RB-PHE. The evaluation of ROU by PHE was performed in the absence of HPβCD, since it was recently reported that the photodegradation rate of PHE displays no differences in the presence or absence of the oligosaccharide [31]. Our results are shown in Fig. 9. As an additional information, a similar set of results from our previous work, performed in methanolic solution, was included in the figure [2]. In all cases, independently of the medium and photosensitizer employed, it can be observed that photooxidation occurs at much

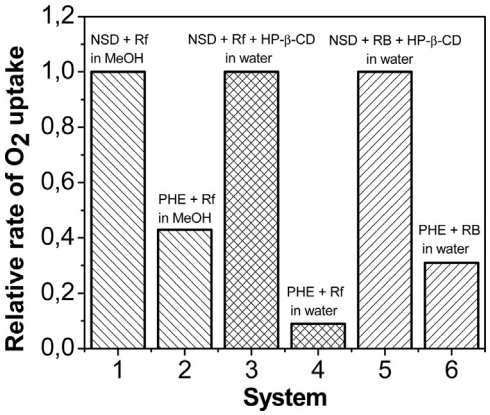

Fig. 9. Bars diagram for the relative rates of oxygen uptake by different systems containing NSD and PHE as photooxidizable substrates and the sensitizers Rf and RB. Systems (1) and (2) are results published in reference [2]. (1) 0.035 mM Rf + 0.45 mM NSD in MeOH; (2) 0.035 mM Riboflavin + 0.45 mM PHE in MeOH (3) Rf-HPβCD + NSD-$(HP\beta CD)_2$ containing 0.07 mM NSD; 0.04 mM Rf and 37 mM HPβCD; (4) 0.07 mM PHE + 0.04 mM Rf; (5) RB-HPβCD + NSD-$(HP\beta CD)_2$ containing 0.04 mM NSD; 0.008 mM RB and 37 mM HPβCD; (6) 0.07 mM PHE + 0.008 mM RB. (3)–(6) are aqueous solutions.

higher rate in the case aqueous HPβCD-NSD systems than in the PHE aqueous solution. It is known that in distilled water PHE is exclusively in its molecular form ($pK_{PHE} = 10$) [32].

4. Discussion

4.1. The inclusion complex of aqueous HPβCD-NSD

The present theoretical studies suggest the formation of an inclusion complex NSD-HPβCD with 1:2 stoichiometry is possible, in excellent agreement with previous experimental results [10]. Because in the 1:2 complex the NSD molecule is completely embedded in both CDs cavities, there are more host-guest interactions than in the 1:1 complex, resulting in a higher stability for the former structure. The assembly NSD + 2 oligosaccharide molecules adopts a so-called head-to-head orientation and is supported by four host-guest intermolecular H-bonds and a weak non-covalent interaction Cl-H.

4.2. Rf-photoinduced oxidation of HPβCD-encapsulated NSD. Electron transfer process and the role of photogenerated ROS

The ROS $O_2(^1\Delta_g)$, $O_2^{\bullet-}$ and H_2O_2, generated through Rf-photosensitization in the presence of HPβCD-encapsulated NSD, effectively react with NSD. The first species is formed through an energy transfer step (Reaction (13)), with a rate constant of $1.1 \times 10^8\ M^{-1}\ s^{-1}$ in aqueous solution [33], whereas the ROS $O_2^{\bullet-}$ and H_2O_2 are produced after electron transfer (step (6)), as an initial step, with a determined ^3k_q value of $5.1 \times 10^7\ M^{-1}\ s^{-1}$. Under similar concentrations of dissolved oxygen both processes are competitive and consequently the respective ROS can be formed.

The ^3k_q value determined in the HPβCD-NSD complex (reaction (2)) was *ca.* two orders of magnitude lower than that obtained for the same excited species-quencher couple in the absence of HPβCD, employing MeOH as a solvent (Table 3) [2]. A similar result has been already observed by Sengupta et al. by comparing the quenching of ^{3}Rf* by triethylamine (TEA) in the presence and in the absence of aqueous β-cyclodextrin. [24] Turning to our case and in line with the reasoning of Sengupta et al. two factors could cooperate for the observed reduction of the electron transfer rate constant value:

Table 3
Rate constant for the electron transfer quenching of HPβCD.Rf by NSD-$(HP\beta CD)_2$. Overall (k_t) and reactive (k_t) rate constants for the quenching of $O_2(^1\Delta_g)$ by NSD-$(HP\beta CD)_2$ in differet media.

Medium	$k_{q3} \times 10^7\ M^{-1}\ s^{-1}$	$k_t \times 10^6\ M^{-1}\ s^{-1}$	$k_r \times 10^6\ M^{-1}\ s^{-1}$
(a) MeOH	930	0.5 ± 0.80	0.5 ± 0.4
(a) MeOH/ 50 mM NaOH	Not determined	8.7 ± 0.8	8.6 ± 0.1
Aqueous NSD-$(HP\beta CD)_2$	5.1 ± 0.2	170 ± 5	24 ± 0.8

(a) From reference [2].

(a) NSD forms an inclusion complex HPβCD whereas Rf forms only an H-bonded complex with the oligosaccharide [8]. This fact could decrease the encounter probability between both electron-transfer candidates as a consequence of a mobility reduction of the encapsulated NSD. The immediate consequence of this fact could be evident by a decrease in the collision frequency between NSD-$(HP\beta CD)_2$ and HPβCD-hydrogen bonded ^{3}Rf*, affecting the efficiency of the electron transfer process.

(b) If the radicals generated in Reaction (6) are not properly stabilized, it is possible an increase of the back electron transfer reaction to regenerate ^{3}Rf* and NSD. It could occur if solvation near HPβCD is reduced enough to produce a retardation in the hydrogen abstraction from water molecules by the initially electron-transferred species Rf-$(HP\beta CD)_2^{\bullet+}$ Rf-(HPβCD)Rf-(HPβCD). Bulky organized assemblies appear as less efficient to form the stabilized neutral radical RfH-$(HP\beta CD)_2^{\bullet}$ than free $Rf^{\bullet+}$ species present in homogeneous MeOH (Reaction (7)).

We think that both factors could simultaneously cooperate in a sort of synergistic effect, in the case of the electron-transfer mediated quenching of the hydrogen bonded ^{3}Rf*-HPβCD by NSD-$(HP\beta CD)_2$. The expected measurable effect is a decrease in the rate constant ^3k_q accounting for the effective electron transfer process.

From Table 3 it can be seen that the rate constants k_t and k_r, representing the quenching processes of $O_2(^1\Delta_g)$ by NSD-$(HP\beta CD)_2$ are considerably higher when the contaminant is encapsulated in the aqueous cyclodextrine system than dissolved in pure MeOH. This result is supported by the mechanistic interpretation of the interaction of electron-releasing derivatives, including phenols, with the electrophilic species $O_2(^1\Delta_g)$. This process involves an intermediate encounter complex possessing some degree of charge-transfer character, represented by Scheme 2. [34–36]

The second line of Scheme 2 includes the complete electron transfer process that will produce irreversible chemical oxidation of NSD. The third line shows the deactivation of the encounter complex leading to physical quenching and yielding the unreacted substrate and ground state molecular oxygen.

The formation and evolution of the encounter complex is highly influenced by solvent polarity and electron releasing ability of the involved substrate. Hence, and turning again to the rate constant values shown in Table 3, the change of solvent from MeOH to water and the presence of a considerable proportion of the electron-donating phenolate form of NSD in the aqueous encapsulated system, justify the mentioned considerable increase in the $O_2(^1\Delta_g)$ rate constant values.

4.3. Comparative experiments between overall NSD- and PHE-photooxidation rates

Fig. 9 clearly shows that the overall rate of oxygen uptake upon Rf-and RB-photosensitization is much faster for aqueous HPβCD-encapsulated NSD than for aqueous PHE. Besides, the ROU for PHE

in the RB-photosensitized system is *ca.* three times higher than that observed for the Rf-photosensitization, in both cases relative to the ROU observed for the systems containing NSD. As said, PHE exhibits a limited reactivity of in its molecular form towards $O_2(^1\Delta_g)$ [37]. This means that the combined action of $O_2^{\bullet}-$, H_2O_2 and $O_2(^1\Delta_g)$ identified as the NSD-$(HP\beta CD)_2$ oxidative ROS, employing Rf as a photosensitizer, constitute an efficient system, as compared to the overall oxidative rate observed for PHE employing the same photosensitizer.

Results of the comparison between overall photooxidation efficiency for the Rf-sensitized systems in MeOH and in aqueous medium are also clear. As shown in Fig. 9, the ROU for aqueous encapsulated NSD is *ca.* five-fold faster that the corresponding one in MeOH, always relative to the ROU of PHE in the respective media. In this case the addition of solvent polarity and ionization effects constitutes the driving force in the increase of the $O_2(^1\Delta_g)$-mediated photodegradation rate of NSD.

5. Conclusions

Theoretical calculations confirm that NSD forms an inclusion complex with HβCD in aqueous solution with a prevalent 1:2 stoichiometry. The NSD molecule is completely embedded in both CDs cavities, in a so called "head-to-head" orientation.

Kinetics of the electron transfer process and oxidation through $O_2(^1\Delta_g)$-mechanism are affected by NSD encapsulation, due to dynamic limitations, electrostatic forces and pH of the oligosaccharide cavity.

The ROS $O_2(^1\Delta_g)$, $O_2^{\bullet-}$ band H_2O_2, generated through Rf-photosensitization in the presence of NSD-$(HP\beta CD)_2$, are effectively intercepted by the encapsulated biocide. The overall ROU upon Rf and RB photosensitization, in the presence of HPβCD is a relatively efficient process as compared with the respective ROU for NSD in MeOH and PHE in water. Solvent polarity effects and ionization of the NSD phenolic group in the NSD-encapsulated system play a dominant role in the ROU enhancement through a $O_2(^1\Delta_g)$-mediated mechanism. The NSD encapsulated system can be seen as a sort of nanoreactor, able to increase the photodegradation efficiency of the biocide under daylight conditions.

Acknowledgements

Financial support from Consejo Nacional de Investigaciones Científicas y Técnicas (CONICET), Agencia Nacional de Promoción Científica y Tecnológica (ANPCyT), Agencia Córdoba Ciencia (ACC), Secretarías de Ciencia y Técnica of the Universidad Nacional de Río Cuarto (SECyT UNRC), of the Universidad Nacional de la Patagonia SJB (SECyT UNP-SJB) and of the Universidad Nacional de San Luis (SECyT UNSL), all from Argentine, is gratefully acknowledged. JN, AP, MIS, WAM and NAG are members of the Scientific Researcher Career of CONICET. Thanks are given to Dr. Isela Guitérrez for helpful assistance in the determination of k_{rR} value in water.

References

[1] C. Tomlin, The Pesticide Manual, British Crop Protection Council and The Royal Society of Chemistry, London, UK, 1994.
[2] J. Natera, E. Gatica, C. Challier, D. Possetto, W. Massad, S. Miskoski, A. Pajares, N. A. García, On the photooxidation of the multifunctional drug niclosamide. A kinetic study in the presence of vitamin B 2 and visible light, Redox Rep. 20 (2015) 259–266.
[3] P.F. Heelis, The photophysical and photochemical properties of flavins (isoalloxazines), Chem. Soc. Rev. 11 (1982) 15–39.
[4] J.P. Escalada, A. Pajares, J. Gianotti, A. Biasutti, S. Criado, P. Molina, W. Massad, F. Amat-Guerri, N.A. García, Photosensitized degradation in water of the phenolic pesticides Bromoxynil and Dichlorophen in the presence of Riboflavin as a model of their natural photodecomposition in the environment, J. Hazard. Mater. 186 (2011) 466–472.
[5] Y. Barbieri, W.A. Massad, D.J. Díaz, J.S.F. Amat-Guerri, N.A. García, Photodegradation of Bisphenol A and related compounds under natural-like conditions in the presence of riboflavin. Kinetics mechanism and photoproducts, Chemosphere 73 (2008) 564–571.
[6] A. Douhal, Cyclodextrins Materials: Photochemistry, Photophysics and Photobiology, 1st ed., Elsevier, Amsterdam, 2006.
[7] N. Singla, P. Chowdhury, Inclusion behavior of infole-7-carboxaldehyde inside β-cyclodextrin. A nano cage, Chem. Phys. 441 (2014) 93–100.
[8] M.L. Ruiz del Castillo, E. López-Tobar, S. Sanchez-Cortes, Gema Flores, G.P. Blanch, Stabilization of curcumin against photodegradation by encapsulation in gamma-cyclodextrin: a study based on chromatographic and spectroscopic (Raman and UV–visible) data, Vib. Spectr. 81 (2015) 106–111.
[9] M. Gmurek, M. Olak-Kucharczyk, S. Ledakowicz, Photochemical decomposition of endocrine disrupting compounds –a review, Chem. Eng. J. 310 (2017) 437–456.
[10] P.J.W. Morrison, C.J. Connon, V.V. Khutoryanskiy, Cyclodextrin-mediated enhancement of riboflavin solubility and corneal permeability, Mol. Pharm. 10 (2013) 756–762.
[11] B. Devarakonda, R.H. Hill, W. Liendebeerg, M. Brits, M.M. de Villiers, Complextion of the aqueous solubilization of practically insoluble niclosamide by polyamideamine (PAMAM) dendrimers nd cyclodextrines, Int. J. Pharm. 304 (2005) 193–209.
[12] F.E. Scully, J. Hoigné, Rate constants for reactions of singlet oxygen with phenols and other compounds in water, Chemosphere 16 (1987) 681–694.
[13] W. Massad, S. Bertolotti, M. Romero, N.A. García, A kinetic study on the inhibitory action of sympathomimetic drugs towards photogenerated oxygen active species. The case of phenylephrine, J. Photochem. Photobiol. B: Biol. 80 (2005) 130–138.
[14] F. Wilkinson, W.P. Helman, A.B. Ross, Rate constants for the decay and reactions of the lowest electronically excited singlet state of molecular oxygen in solution. an expanded and revised compilation, J. Phys. Chem. Ref. Data 24 (1995) 663–677.
[15] J.J.P. Stewart, Optimization of parameters for semiempirical methods V: modification of NDDO approximations and application to 70 elements, J. Mol. Model. 13 (2007) 1173–1213.
[16] A.J. Sharff, L.E. Rodseth, F.A. Quiocho, Refined 1.8-A structure reveals the mode of binding of beta-cyclodextrin to the maltodextrin binding protein, Biochemistry (Mosc.) 32 (1993) 10553–10559.
[17] M.I. Sancho, M.G. Russo, M.S. Moreno, E. Gasull, S.E. Blanco, G.E. Narda, Physicochemical characterization of 2-hydroxybenzophenone with β-cyclodextrin in solution and solid state, J. Phys. Chem. B 119 (2015) 5918–5925.
[18] S. Dapprich, I. Komáromi, K.S. Byun, K. Morokuma, M.J. Frisch, A new ONIOM implementation in Gaussian98. Part I. The calculation of energies, gradients, vibrational frequencies and electric field derivatives1, J. Mol. Struct. Theochem. 461–462 (1999) 1–21.
[19] M.J. Frisch, G.W. Trucks, H.B. Schlegel, G.E. Scuseria, M.A. Robb, J.R. Cheeseman, G. Scalmani, V. Barone, B. Mennucci, G.A. Petersson, et al., Gaussian 09, Revision D.01, Gaussian, Inc., Wallingford CT, 2009.
[20] A.E. Reed, L.A. Curtiss, F. Weinhold, Intermolecular interactions from a natural bond orbital donor-acceptor viewpoint, Chem. Rev. 88 (1988) 899–926.
[21] M.I. Sancho, E. Gasull, S.E. Blanco, E.A. Castro, Inclusion complex of 2-chlorobenzophenone with cyclomaltoheptaose (β-cyclodextrin): temperature, solvent effects and molecular modeling, Carbohydr. Res. 346 (2011) 1978–1984.
[22] E. Engeldinger, D. Armspach, D. Matt, P.G. Jones, R. Welter, A cyclodextrin diphosphane as a first and second coordination sphere cavitand: evidence for weak C-H···Cl-M hydrogen bonds within metal-capped cavities, Angew. Chem. Int. Ed. 41 (2002) 2593–2596.
[23] (Hydroxypropyl)-γ-cyclodextrin779229. http://www.sigmaaldrich.com/catalog/product/aldrich/779229, 2017 (accessed: 21st April).
[24] C. Sengupta, M.K. Sarangi, A. Sau, D. Mandal, S. Basu, A case study of photo induced electron transfer between riboflavin and aliphatic amine: deciphering different mechanisms of ET operating from femtosecond to microsecond time domain, J. Photochem. Photobiol. Chem. 296 (2015) 25–34.
[25] E. Haggi, S. Bertolotti, N.A. Garcı'a, Modelling the environmental degradation of water contaminants. Kinetics and mechanism of the riboflavin-sensitised-photooxidation of phenolic compounds, Chemosphere 55 (2004) 1501–1507.
[26] F. Amat-Guerri, M.M.C. López-González, R. Martínez-Utrilla, R. Sastre, Singlet oxygen photogeneration by ionized and un-ionized derivatives of Rose Bengal and Eosin Y in diluted solutions, J. Photochem. Photobiol. Chem. 53 (1990) 199–210.
[27] P. Fini, M. Castagnolo, L. Catucci, P. Cosma, A. Agostiano, Inclusion complexes of Rose Bengal and cyclodextrins, Thermochim. Acta 418 (2004) 33–38.
[28] E. Silva, A.M. Edwards, D. Pacheco, Visible light-induced photooxidation of glucose sensitized by riboflavin, J. Nutr. Biochem. 10 (1999) 181–185.
[29] E. Silva, L. Herrera, A.M. Edwards, J. de la Fuente, E. Lissi, Enhancement of riboflavin-mediated photo-oxidation of glucose 6-phosphate dehydrogenase by urocanic acid, Photochem. Photobiol. 81 (2005) 206–211.
[30] J.P. Escalada, A. Pajares, J. Gianotti, W.A. Massad, S. Bertolotti, F. Amat-Guerri, Dye-sensitized photodegradation of the fungicide carbendazim and related benzimidazoles, Chemosphere 65 (2006) 237–244.
[31] Y. Zhou, X. Gu, R. Zhang, J. Lu, Influences of various cyclodextrins on the photodegradation of phenol and bisphenol A under UV light, Ind. Eng. Chem. 54 (2015) 426–433.

[32] C.D. Hodgman, R.C. Weast, R.S. Shankland, S.M. Selby, Handbook of Chemistry and Physics, 44th ed., Chemical Rubber Pub. Co., Cleveland, OH, 1963.
[33] M. Koizumi, S. Kato, N. Mataga, T. Matsuura, I. Isui, Photosensitized Reactions, Kagakudogin Publishing Co, Kyoto, Japan, 1978, pp. 218–219.
[34] C. Tanielian, C. Wolf, Mechanism of physical quenching of singlet molecular oxygen by chlorophylls and related compounds of biological interest, Photochem. Photobiol. 48 (1988) 277–280.
[35] A.A. Gorman, I. Hamblett, C. Lambert, Identification of both preequilibrium and diffusion limits for reaction of singlet oxygen, O_2 ($^1{}_g$), with both physical and chemical quenchers: variable-temperature, time-resolved infrared luminiscence studies, J. Am. Chem. Soc. 110 (1988) 8053–8059.
[36] A.A. Gorman, I.R. Gould, I. Hamblett, M.C. Standen, Reversible exciplex formation between singlet oxygen, $^1\Delta_g$, and vitamin E Solvent and temperatures effects, J. Am. Chem. Soc. 106 (1984) 6956–6959.
[37] N.A. García, Singlet molecular oxygen-mediated photodegradation of aquatic phenolic pollutants. A kinetic and mechanistic overview, J. Photochem. Photobiol. B: Biol. 22 (1994) 185–196.